

Characteristics of Temperature Change in China over the Last 2000 years and Spatial Patterns of Dryness/Wetness during Cold and Warm Periods

Quansheng GE^{1,2}, Haolong LIU¹, Xiang MA¹, Jingyun ZHENG^{1,2}, and Zhixin HAO^{*1,2}

¹*Key Laboratory of Land Surface Pattern and Simulation, Institute of Geographic Sciences and Natural Resources Research, Chinese Academy of Sciences, Beijing 100101, China*

²*University of Chinese Academy of Sciences, Beijing 100049, China*

(Received 18 October 2016; revised 7 March 2017; accepted 14 March 2017)

ABSTRACT

This paper presents new high-resolution proxies and paleoclimatic reconstructions for studying climate changes in China for the past 2000 years. Multi-proxy synthesized reconstructions show that temperature variation in China has exhibited significant 50–70-yr, 100–120-yr, and 200–250-yr cycles. Results also show that the amplitudes of decadal and centennial temperature variation were 1.3°C and 0.7°C, respectively, with the latter significantly correlated with long-term changes in solar radiation, especially cold periods, which correspond approximately to sunspot minima. The most rapid warming in China occurred over AD 1870–2000, at a rate of $0.56^\circ \pm 0.42^\circ \text{C} (100 \text{ yr})^{-1}$; however, temperatures recorded in the 20th century may not be unprecedented for the last 2000 years, as data show records for the periods AD 981–1100 and AD 1201–70 are comparable to the present. The ensemble means of dryness/wetness spatial patterns in eastern China across all centennial warm periods illustrate a tripole pattern: dry south of 25°N, wet from 25°–30°N, and dry to the north of 30°N. However, for all centennial cold periods, this spatial pattern also exhibits a meridional distribution. The increase in precipitation over the monsoonal regions of China associated with the 20th century warming can primarily be attributed to a mega El Niño–Southern Oscillation and the Atlantic Multidecadal Oscillation. In addition, a significant association between increasing numbers of locusts and dry/cold conditions is found in eastern China. Plague intensity also generally increases in concert with wetness in northern China, while more precipitation is likely to have a negative effect in southern China.

Key words: temperature change, dry-wet spatial pattern, cold and warm periods, last 2000 years, China

Citation: Ge, Q. S., H. L. Liu, X. Ma, J. Y. Zheng, and Z. X. Hao, 2017: Characteristics of temperature change in China over the last 2000 years and spatial patterns of dryness/wetness during cold and warm periods. *Adv. Atmos. Sci.*, **34**(8), 941–951, doi: 10.1007/s00376-017-6238-8.

1. Introduction

Knowledge about past climate can improve our understanding of natural climate variability and help us to address the question of whether modern climate change is unprecedented in a long-term context. The Intergovernmental Panel on Climate Change (IPCC, 2013) reported that average annual Northern Hemisphere (NH) temperatures over the period between 1983 and 2012 mean that this was very likely the warmest 30-year period in the last 800 years (a result that has high statistical confidence), and perhaps the warmest 30 years seen in the last 1400 years (a result that has medium statistical confidence). In addition, data show that the probability of drought occurrence has increased over the last millennium, while those that do take place have great magnitude and longer duration in many regions than have been observed

since the beginning of the 20th century. Data have also been presented that indicate more mega-droughts have occurred in monsoonal Asia and that wetter conditions have prevailed in arid Central Asia and in the South American monsoonal region since the Little Ice Age (LIA—the period between AD 1450 and AD 1850) compared to the Medieval Climate Anomaly (MCA—the period between AD 950 and AD 1250).

Continental-scale surface temperature reconstructions have been used with high confidence to demonstrate that there were multi-decadal periods during the MCA when some regions were as warm as the mid-20th century, and other times when temperatures were as high as in the late 20th century (IPCC, 2013; PAGES 2k Consortium, 2013). However, the absence of widespread instrumental climate records for periods earlier than the 20th century necessitates the use of natural climate archives or “proxy” data (e.g., tree rings, corals, ice cores, historical documentary records) for past climate reconstruction (NRC, 2006; Ge et al., 2010). Because

* Corresponding author: Zhixin HAO
Email: haozx@igsnrr.ac.cn

these approaches involve numerous uncertainties at regional scales, it is important to evaluate differences in amplitude and trends, as well as the variability of individual reconstructions, to describe the main sources of uncertainty, as well as to summarize the effects of the choice of proxy data and statistical calibration methods. This approach is particularly important for regional reconstructions if our aim is to address whether warming observed over the 20th century is exceptional given the context of the past. This is especially important in China—a country with various climatic zones—when we study the climate changes in China for the past 2000 years (hereafter abbreviated to “CCCP2k” for convenience) (Lü and Ding, 2012; Liao et al., 2016). As a result of studying CCCP2k, a large volume of high-resolution proxies, paleoclimatic reconstructions, and new results have been generated over the last five years. The key insights from this research are summarized in this paper.

2. New climate proxies and temperature reconstructions achieved from CCCP2k

2.1. Collection of new climate proxies

More than 30 000 individual meteorological (e.g., phenological cold and warm events, snowfall days, plant phenodates, drought and flood events) and 7367 zoological records (e.g., locust plagues, large mammal range contractions) have been extracted from Chinese historical documents over the last five years. In addition, new samples from natural archives have been collected, comprising more than 1000 tree-ring cores from the Tibetan Plateau (TP) and Taiwan (Fig. 1); three ice cores of lengths 170 m, 189 m, and 110 m from the northern, central, and southern TP, respectively;

six millennium-scale stalagmites from caves at Kesang ($42^{\circ}52'N$, $81^{\circ}45'E$), Shihua ($39^{\circ}47'N$, $115^{\circ}56'E$), Huangye ($33^{\circ}35'N$, $105^{\circ}7'E$), Huanglong ($32^{\circ}43'N$, $103^{\circ}49'E$), Heilong ($31^{\circ}36'N$, $110^{\circ}51'E$), and Shennong ($28^{\circ}42'N$, $117^{\circ}15'E$); 30 sediment cores from lakes Sihailongwan Maar [($42^{\circ}17'N$, $126^{\circ}36'E$), 791 m above sea level (ASL)], Ku-sai [$(35^{\circ}37'-35^{\circ}50'N$, $92^{\circ}38'-93^{\circ}15'E$), 4475m ASL], Zige-tang Co [$(32^{\circ}00'-32^{\circ}09'N$, $90^{\circ}44'-90^{\circ}58'E$), 4560 m ASL], and Huguang Maar ($21^{\circ}9'N$, $110^{\circ}17'E$); 500 m long coral cores from more than 300 massive *Porites* colonies; nine lagoonal sediment cores; and more than 20 *Tridacna* specimens from the South China Sea (Sun et al., 2013; Tao et al., 2016). Based on these proxies, 25 new paleoclimatic reconstructions have been generated, including seven well-dated $\delta^{18}\text{O}$ series from stalagmites. Some of these reconstructions have already been published (Ge et al., 2016), while eight cover the last 2000 years, two cover the last 1500 years, nine cover the last 1000 years, and others encompass the last 500 years.

2.2. New reconstructions of temperature change

A new 2000-year multi-proxy synthesized reconstruction for temperature change across China at decadal resolution is shown in Fig. 2. This reconstruction was derived from sub-regional proxy temperature data (Ge et al., 2013a), encompassing 28 series for the whole country, most of which have a finer than 10-year temporal resolution. Compared with earlier synthesized temperature reconstructions for China (e.g., Yang, 2002; Wang et al., 2007), which employed temperature proxies from individual sites, the new reconstruction has wide spatial coverage because the proxies used come from numerous sites and are mostly novel. In addition, this reconstruction was generated using a new synthetic approach; in the first place, each sub-regional proxy temperature series was developed using an envelope assessment to capture regional signals with maximum confidence (Ge et al., 2010), employing a range of proxies (e.g., historical documents, tree rings, ice cores, lake sediments, and stalagmites) from individual sites or small regions. The observed national temperature series for the period between AD 1871 and AD 2000 (released by the China Meteorological Administration; Tang et al., 2010) was used for calibration, and two regression methods (principal component regression and partial least-squares regression incorporating “leave-one-out” cross-validation) were adopted to calibrate the sub-regional proxy and national temperature, respectively. Thus, the degree of confidence in the results is improved by cross-verification of two reconstructions.

Ten new temperature reconstructions for sub-regions or individual sites generated during CCCP2k studies are shown in Fig. 3, while the metadata for these are listed in Table 1. For these 10 reconstructions, three sub-regional series (i.e., northeastern, central eastern China, and the TP), at decadal resolution, were synthesized from individual temperature reconstructions or proxies using an envelope assessment to capture the highest-confidence signals for calibration (Ge et al., 2013a). The other seven reconstructions, with annual resolution, were derived using historical documents and tree rings.

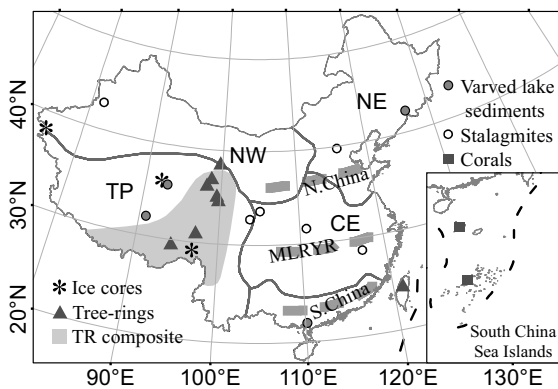


Fig. 1. Locations for the main new proxy samples collected from natural archives and regional divisions (northeast, NE; central east, CE; South China, SC; northwest, NW) used for synthesized multi-proxy temperature reconstruction. The bold gray dashed lines show North China, the MLRYR and South China, respectively, used for temperature reconstructions from historical documents, while the gray area shows the region of the eastern TP that was used for tree-ring (TR) composite temperature reconstruction.

Table 1. The ten temperature reconstructions for sub-regions and individual sites illustrated in Fig. 3.

No.	Sub-region/site	Lon. ($^{\circ}$ E)	a.s.l. (m)	Period Resolution	Proxy	Target reconstructed	Method*	Reference
W1	Qilian Mountains	99.67–99.70 38.69–38.72	3300–3578	AD 670–2012 Annual	Tree-ring width from four sites with 64, 80, 24, and 82 cores	Mean minimum temperature from January to August	Negative exponential curve and linear curve with negative slope	Zhang et al. (2014)
W2	TP	75–104 22–39		AD 1–2000 Decadal	Five ice cores, one tree-ring width, and two lake sediments	Decadal mean temperature	Envelope assessment to capture the highest-confidence signal for calibration	Ge et al. (2013a)
W3	Animaqin Mountains	99.45–99.47 35.17–35.22	3900–4100	261 BC to AD 2012 Annual	Tree-ring width from four sites with 119, 25, 67, and 42 cores	Mean maximum temperature from April to June	Smoothing splines with 50% frequency cutoff at 67% of the curve length	Chen et al. (2016)
W4	Eastern TP	87–102 27–38	3100–4500	AD 1000–2005 Annual	12 tree-ring width chronologies	Mean temperature from June to August	Composite plus scale approach	Wang et al. (2015)
W5	Bomi-Linzhi	96.50–96.77 29.45–29.57	3982–4329	AD 1385–2002 Annual	Tree-ring width from five sites with 60, 42, 51, 53, and 45 cores	Mean minimum temperature of August	Regional curve standardization	Zhu et al. (2011)
E1	Northeast China	110–125 38–55		AD 1–2000 Decadal	Five reconstructions comprising two from documents, two from sediments, one from a stalagnite	Decadal mean temperature	Envelope assessment to capture the highest-confidence signal for calibration	Ge et al. (2013a)
E2	Central East China	East of 105 25–38		AD 1–2000 Decadal	Phenological events from historical documents	Decadal mean temperature of October to April	Phenology–temperature regression and spatial representativeness synthesis	Ge et al. (2003, 2013a)
E3	North China	East of 105 33–42		AD 1501–2010 Annual	Phenological events from historical documents	Mean temperature from October to April	Phenology–temperature regression and spatial representativeness synthesis	Yan (2014)
E4	MLRYR	East of 105 26–33		AD 1501–2010 Annual	Phenological events from historical documents	Mean temperature from October to April	Phenology–temperature regression and spatial representativeness synthesis	Yan (2014)
E5	South China	East of 105 South of 26		AD 1501–2009 Annual	Phenological events from historical documents	Mean temperature from November to February	Phenology–temperature regression and envelope analysis	Zheng et al. (2016)

*For tree-ring-based reconstruction, the method involves removing age-related trends only, as all tree-ring based reconstructions are calibrated by regression between tree rings and temperature.

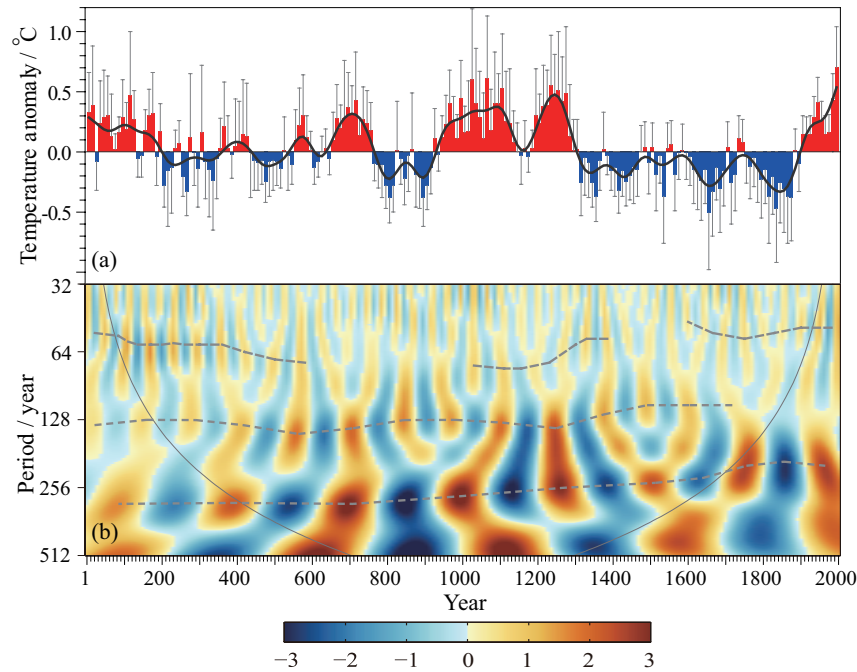


Fig. 2. (a) A 2000-year temperature reconstruction for China synthesized from 28 proxies or individual reconstructions, along with the (b) Morlet wavelet spectrum. The dashed line indicates significant multidecadal to centennial cycles and the solid line indicates the cone of influence.

Of these, four reconstructions derived from tree rings (Fig. 3; W1, W3–5) augment the sparse number of millennial-scale yearly temperature records for western China, and include the longest reconstruction for the Animaqin Mountains extending back to 261 BC. The reconstruction for the Qilian Mountains also provides a millennial-scale annual temperature record for northwestern China and provides a good spatial representation of temperature change for not just the TP, but across most of northwestern China. At the same time, three new temperature series—for northern China, the mid-lower reaches of the Yangtze River (MLRYR), and southern China (Fig. 3; E3–E5)—improve the available temporal resolution of documentary-based temperature reconstructions for eastern China over the past 500 years from decadal to annual. These series thus provide very important temperature data for further studying the long-term effects of extreme climate events (Zheng et al., 2014a; Qin et al., 2015; Ge et al., 2016), as well as the sensitivity of climate warming to changes in CO₂ concentration (Liao et al., 2016). It is worth noting that, although most of the series in Table 1 show seasonal temperature changes rather than annual temperature, the annual temperature signal is also included and, in fact, even explains the variation to a greater extent. For example, for the correlation coefficients between seasonal and annual temperature corresponding to the observed data from 1951 to 2014, the minimum is 0.45 and the maximum is 0.94, all passing the 0.01 significance level, in which lower correlation is likely for the summer and higher correlation for winter.

In addition, based on the thickness of the light layer iden-

tified in varved sediments from Lake Kusai, estimates for summer temperatures over the period 350–2010 on the northern TP have been generated (Liu et al., 2014). Based on long-chain alkenones extracted from these varved sediments, the variability in the surface temperature of Lake Sihailongwan Marr (northeastern China) for the growing season over the last 1600 years has also been estimated (Chu et al., 2011); while using the ratio of strontium to calcium derived from coral cores around the Xisha Islands in the South China Sea, the sea surface temperature (SST) for the period AD 1458 to AD 2015 has been reconstructed (Tao et al., 2016). Specifically, Tan (2014, 2016) analyzed variations in stalagmite δ¹⁸O across the monsoonal region of China to reconstruct the tropical Pacific SST gradient. As large-scale El Niño–Southern Oscillation (ENSO)-like states occurring over the last millennium have thus been reconstructed using oxygen isotope records from Chinese stalagmites (Tan, 2014, 2016), these studies provide important evidence enabling further investigation of the possible ways these conditions can control climate change in the monsoonal regions of China over interannual, centennial, and longer timescales.

3. Results and discussion

3.1. Temperature change characteristics

Results show that temperature change in China over the last 2000 years is characterized by four warm epochs and four cold periods on the centennial timescale (Fig. 2; the reference

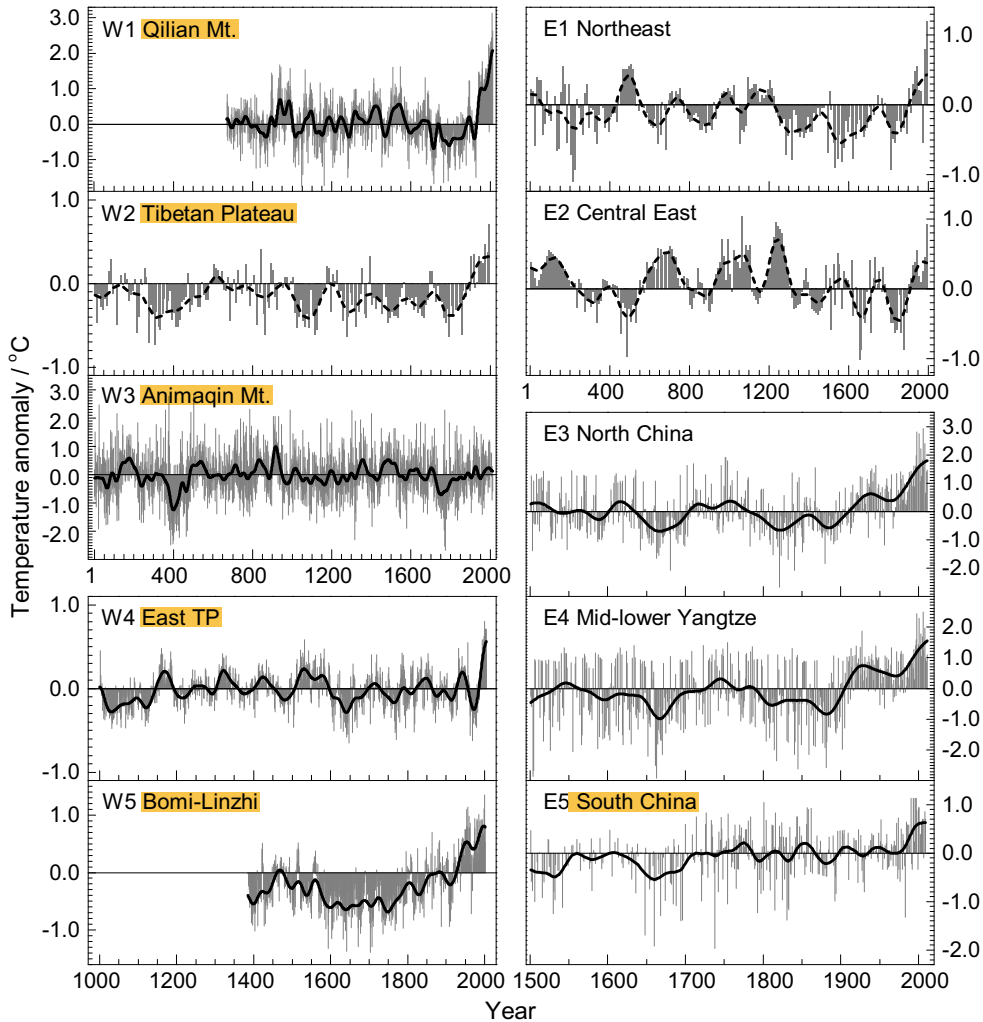


Fig. 3. Ten new temperature reconstructions for sub-regions of China at decadal resolution, as well as individual sites at annual resolution, for the last 2000 years, with the mean value of 1851–1950 as the base period. Information on each series can be found in Table 1.

climatology is the mean value from 1851 to 1950). Data show that the warm epochs occurred during the periods AD 1 to AD 200, AD 550 to AD 760, AD 950 to AD 1300, and during the 20th century, while cold periods occurred between AD 210 and AD 350, AD 420 and AD 530, AD 780 and AD 940, and AD 1320 and AD 1900. Temperature amplitudes from the warmest and coldest decades and centuries over the last 2000 years are 1.3°C and 0.7°C , respectively. Meanwhile, comparison of warmth levels in the 20th century shows that temperatures in the warmest 100 years (the period between AD 31 and AD 130) and 30 years (the period between AD 91 and AD 120) over the period between AD 1 to AD 200 are a little lower, while temperatures in the warmest 100 years (the period between AD 661 and AD 760) and 30 years (the period between AD 691 and AD 720) between AD 550 and AD 760 are similar. In contrast, temperatures in the warmest 100 years (the period between AD 1191 and AD 1290) and

30 years (the period between AD 1231 and AD 1260) between AD 950 and AD 1300 are higher. Results also show that the extent of warming seen during the 20th century is not unprecedented over the last 2000 years; the warmth level of the period AD 1231 to AD 1260 during the MCA is comparable to the present day. Rates of temperature change on the centennial timescale suggest that rapid warming occurred between AD 1870 and AD 2000 [a rate of $0.56^{\circ} \pm 0.42^{\circ}\text{C}$ (100 yr) $^{-1}$ at the 95% confidence level] (Ge et al., 2013a). This rate of temperature change is not particularly unique, as similar periods characterized by rapid warming also occurred in the periods between AD 600 and AD 710 [$0.51^{\circ} \pm 0.45^{\circ}\text{C}$ (100 yr) $^{-1}$], AD 880 and AD 990 [$0.65^{\circ} \pm 0.43^{\circ}\text{C}$ (100 yr) $^{-1}$], and AD 1150 and AD 1250 [$0.63^{\circ} \pm 0.42^{\circ}\text{C}$ (100 yr) $^{-1}$]. Results show that, over the last 2000 years, temperature change in China has cycles of 50 to 70 years, 100 to 120 years, and 200 to 250 years (Fig. 2b); and of these, the quasi-200-year

cycle is in close agreement with solar activity, with the exception of the period between AD 950 and AD 1150 (Wang et al., 2014). Indeed, if we compare these data to the occurrence of sunspot minima over the last 2000 years (Muscheler et al., 2004; Steinhilber et al., 2009; Lean, 2010; Delaygue and Bard, 2011; Vieira et al., 2011; Clette et al., 2014), a clear relationship can be detected. When the Wolf (AD 1280 to AD 1350), Spörer (AD 1460 to AD 1550), Maunder (AD 1645 to AD 1715), and Dalton Minimum (AD 1795 to AD 1823) occurred, temperatures in China were lower than during other periods. It is also worth noting that switches in climate from warm to cold may also be linked with volcanic activity, as the number of large eruptions (Volcanic Explosivity Index ≥ 4) increased after the 14th century, while temperature from the MCA onwards entered a long-lasting cold period (Ge et al., 2015).

However, in comparison with the warmth of the 20th century, the warmest intervals have varied among sub-regions of China over the last 2000 years. In northeastern China, the temperature of the warmest 100-year period (AD 441 to AD 540) was similar to the 20th century; while in central eastern China, present-day temperatures are lower than the period AD 1201 to AD 1300, when the warmest period in this region occurred (Ge et al., 2013a), and the amplitude on the centennial timescale reached 1.2°C . Over the TP and in northwestern China, 20th century temperatures have exceeded those of the warmest centuries in these regions (Shao, 2012; Wang et al., 2014; Zhang et al., 2014), while the periodicity analysis presented in Table 2 shows that most regional temperature reconstructions exhibit 20–30-year, 50–70-year, 100–120-year, and 200–250-year cycles. Additional cycles, including 12-year, 40-year, 500-year, 600-year, and 700-year cycles, can also be occasionally detected in some reconstructions. In addition, there are regional differences over China, and the regional temperature series are not in phase all the time during the last 2000 years. On the centennial time scale, the MCA first began in the TP region from the 850s, and then moved to the central eastern region from the 920s, and the northeastern region from the 970s. Even for the present warming period, this began in the TP and northwestern regions in the 1850s, followed later by the northeastern, southeastern and central eastern regions. It is worth noting that each reconstructed series is affected by calibration because of the limited length of the instrumental record.

Although several of the regional temperature changes across China over the last 2000 years are unique, cold and warm epochs across the whole country are consistent with those seen over the NH when compared to the same reference of the 1851–1950 mean value. Results show that the climate was warm during the period AD 1 to AD 270, before entering a cold phase between AD 271 and AD 840 that was nevertheless characterized by temperature fluctuations, based on new NH reconstructions. Subsequently, China entered a warm phase between AD 841 and AD 1290, experienced another cold period between AD 1291 and AD 1910, and has been warm again since AD 1911. Indeed, these characteristics are consistent across the whole country, with the exception of the

period AD 551 to AD 940. Between AD 950 and AD 1300, China experienced two successive warm temperature peaks: one around AD 1080 and one around AD 1250; whereas, just one warm peak around AD 1060 occurred across the NH. The majority of NH and Chinese temperature reconstructions suggest that the warmest 100- and 30-year periods during the MCA were the same, or higher, than those of the 20th century (Ge et al., 2015).

The IPCC (IPCC, 2013) also reported that the period between AD 1982 and AD 2012 was very likely the warmest 30 years in the NH over the last 800 years (a result that has high statistical confidence), and probably for the last 1400 years (a result that has medium statistical confidence). However, viewed at the continental scale, several regions or areas during the MCA experienced similar warming over multi-decadal timescales to that which occurred in the middle to late part of the 20th century (a result that has high statistical confidence; IPCC, 2013). This suggests that, before the 20th century, regional differences in global warming were driven by natural climate forcing—perhaps because the MCA and other epochs with elevated temperatures were warmed by increased solar radiation and were dominated by the thermostat and associated stronger gradient patterns; whereas, global warming in the 20th century was driven by increased greenhouse gas volumes, leading to increased atmospheric stability, weaker zonal circulation, and an associated weaker SST gradient, which characterizes the greenhouse-gas mode. Thus, warming due to increased volumes of greenhouse gases generates a different climate signature from that caused by changes in solar radiation, as demonstrated by results based on an ECHO-G climate model simulation (Liu et al., 2013), and has led synchronized global warming throughout the 20th century, especially in the NH.

In addition, results show that most extreme cold winter events occurred in cold stages; for example, during the low temperature troughs between AD 220 and AD 580 and between AD 1500 and AD 1900, more severe cold winter events occurred, at increased intensities, since AD 1950. Nevertheless, several extreme cold winter events have also been detected during warm climate stages, although the areas impacted were different to those in cold climate stages (Hao et al., 2011). For example, over the last 500 years, China has experienced four extreme snow events comparable in severity and spatial disaster distribution to the event in early 2008; namely, in AD 1578, AD 1620, AD 1796, and AD 1841. Interestingly, all these events correspond to transition points when the climate switched from warm into a multi-decadal cold interval. The NH is generally experiencing a 20-year continuous decrease in temperature, which corresponds to the extreme events of AD 1578, AD 1620, and AD 1796; while subsequently, climate entered a cold phase lasting 30 to 50 years. These results may suggest that extreme cold events, such as the 2008 storm, may provide a significant early warning signal for decadal-scale temperature transitions. Also, they may indicate that the current warming hiatus and frequency of extreme cold events are early climate signals for a switch from warm to multi-decadal cold conditions driven by

Table 2. Significant cycles in multi-decadal to centennial variations detected using proxies or proxy-based temperature reconstructions.

Proxy basis; region	Duration	20–30 yr	50–70 yr	100–120 yr	200–250 yr	Other	Reference
Multi-proxy; China	1–2000		*	*	*	600 yr	This paper
Multi-proxy; NE	1–2000			*	*	400 yr	Ge et al (2013b).
Varved lake sediments; NE	400–2000		*	*	*		Chu et al. (2013)
Historical documents; CE	1–2000				*	600 yr	Ge et al. (2013b)
Historical documents; NC	1500–2000			*			Yan (2014)
Historical documents; MLRYR, East China	1500–2000			*			Yan (2014)
Historical documents; MLRYR, East China	1736–2000	*	*				Hao et al. (2015)
Coral, SST; South China Sea	1458–2015	*		*		12 yr	Tao et al. (2016)
Tree ring; Qilian Mountains, NW	670–2012	*	*	*		500 yr	Zhang et al. (2014)
Tree ring; Qilian Mountains, NW	1560–2011				*	40 yr	Yang et al. (2013)
Multi-proxy; TP	1–2000				*		Ge et al. (2013b)
Tree ring; Animaqin Mountains, northeastern TP	261 BC to AD 2012	*	*	*			Chen et al. (2016)
Ice core $\delta^{18}\text{O}$; central TP	Since 7500 BP				*	750 yr	Duan et al. (2012)
Tree ring; central TP	1480–2010		*				He et al. (2014)
Tree ring composite; East TP	1000–2005		*	*		150 yr	Wang et al. (2015)
Tree ring; East TP	1506–2010	*		*			Xiao et al. (2015)
Tree ring; East TP	1701–2010	*				40 yr	Li et al. (2014)
Tree ring; East TP	1506–2008	*		*		12 yr	Xiao et al. (2013)
Stalagmite $\delta^{18}\text{O}$, $\delta^{13}\text{C}$; Heilong Cave, East TP	790–1780			*			Cui et al. (2012)

*Denotes detected cycle; NE, northeastern China; CE, central eastern China; NC, North China; NW, northwestern China.

natural variability (Ge et al., 2015).

3.2. Spatial patterns in dryness and wetness in cold and warm periods

Reconstructions show that the interactions between temperature variation and precipitation change may be complex and diverse, and that no fixed spatial pattern in anomalies of the latter during either cold or warm periods across eastern China can be detected over the last 2000 years (Hao et al., 2016). Nevertheless, it is possible to identify spatial patterns within five distinct cold intervals: AD 440 to AD 540, AD 780 to AD 920, AD 1390 to AD 1460, AD 1600 to AD 1700, and AD 1800 to AD 1900. Of these, between AD 440 and AD 540, when the upper and middle reaches of the Yellow River and the northern section of the southern Yangtze River were experiencing dry conditions, areas of the Yangtze–Huaihe River in northern China were characterized by wet conditions; whereas, between AD 780 and AD 920, precipitation followed a dry–wet–dry distribution from southeast to northwest, into the middle region of the northern Chinese plain and the middle reaches of the Yangtze River. Between AD 1390 and AD 1460, a spatial pattern of dry conditions in western China and wet conditions in eastern China, bounded by 115°E, is dominant; whereas, between AD 1600 and AD 1700, this spatial pattern in precipitation is reversed, characterized by dry conditions in the east, wet in the middle regions (bounded by 110°E), and dry conditions in the west, meridionally—although the area south of the Yangtze River remained wet. Finally, between AD 1800 and AD 1900, with the exception of Guizhou in the Hanshui

valley, as well as scattered areas of northern China, the climate across the country remained dry (Hao et al., 2016).

Similarly, spatial patterns in wet and dry climate can also be identified for four distinct warm periods. Between AD 650 and AD 750, the eastern part of northwest China and the Yangtze–Huaihe River valley both experienced dry conditions, while the middle and lower reaches of the Yellow River and the area south of the Yangtze River both experienced wet conditions. Between AD 1000 and AD 1100, the spatial distribution was characterized by wet conditions to the south of the Yangtze River and in the eastern part of southwestern China, while dry areas occurred between 28°E and 37°E and wet regions encompassed Hebei Province and most of Shanxi Province, from south to north in the area east of 105°E, while dry conditions prevailed west of 105°E. In the period between AD 1190 and AD 1290, precipitation anomalies were characterized by dry conditions in northern China and wet conditions in the south, generally bounded by 30°N, while the western part of the southern Yangtze River experienced dry conditions and the Hanshui valley was wet. Finally, between AD 1900 and AD 2000, the spatial pattern of precipitation followed a zonal distribution from south to north, as southern China remained dry, south of the Yangtze River was wet, the Huaihe River valley and the North China Plain were both dry, and the eastern part of northwestern China was wet. Comparison of these four warm periods show that, although spatial patterns are different, the key characteristics of dry conditions to the north of the Yangtze River and wet conditions to the south can be seen (Hao et al., 2016). Indeed, the spatial patterns in precipitation anomalies for warm peaks

on the decadal timescale, including AD 691 to AD 720, AD 1231 to AD 1260, AD 1741 to AD 1770, AD 1921 to AD 1950, and AD 1981 to AD 2000, indicate that northern China remained dry overall, while eastern China experienced wet conditions in the period between AD 1741 to AD 1770, during the LIA (Hao et al., 2012).

To further understand the dominant spatial pattern in precipitation anomalies during warm and cold periods, we calculated ensemble means (Fig. 4). Results show that, in cold periods, this spatial pattern exhibits a meridional distribution bounded by 115°E: wet conditions in eastern China but alternating wet and dry conditions in the west. In contrast, during warm periods, this distribution exhibits a zonal distribution: dry conditions to the south of 25°N, wet conditions in the region between 25°N and 30°N, and dry conditions north of this boundary, with the exception of the Loess Plateau. It is worth noting that these characteristics are very similar to those seen during the 20th century, while our data reveal (Fig. 4c) that the probability of dry conditions in northern China corresponding with wet conditions in the south in the Xiangjiang and Ganjing valleys, is likely to increase as the climate transitions from a cold to a warm regime (Zheng et al., 2014b).

Reconstruction of the regional dry–wet index since AD 500 shows that the dominant cycles of decadal variation in summer precipitation are 22–24 yr and quasi-70 yr over the North China Plain; 32–36 yr, 44–48 yr, and quasi-70 yr over the Changjiang–Huaihe River valley; and 32–36 yr and 44–48 yr in the Jiang-Nan area (Zheng et al., 2017). Similar cycles were also detected in a May–September Beijing precipitation reconstruction (Lan et al., 2015) and in the Mei-yu series (Hao et al., 2015), derived from historical documents encompassing the last 300 years. Precipitation reconstruction based on varved lake sediments also highlights dominant cycles of 53–55 yr, 87–89 yr, and 105–110 yr, for northeastern China, over the last 1300 years (Chu et al., 2013).

An important recent study on the NH summer monsoonal

system was carried out by Wang et al. (2013), who showed that this system is characterized by substantial intensification as well as Hadley and Walker circulations. Summer monsoonal precipitation in the NH has increased by 9.5% with each degree of global warming, an intensification that can primarily be attributed to mega-ENSO [like ENSO but with a larger spatial scale and interannual–interdecadal time scale, as defined by Wang et al. (2013)] and the AMO.

3.3. Impact of climate change on locusts and plagues

The anomalous temperature and precipitation changes during the past 200 years have had great impacts on animal migration, insect outbreaks and infectious diseases after major natural disasters. Some research has suggested that the occurrence of locusts and other plagues can be closely associated with climate change, an important issue in global change research (IPCC, 2007; Tian et al., 2011). Thus, the frequency of occurrences of locust and human plagues and their association with climate change based on long-term data recorded in Chinese historical documents were investigated. The reconstruction of outbreaks of oriental migratory locusts (*Locusta migratoria manilensis*) in China over the last 1910 years shows that statistically significant correlations exist between reconstructed locust abundance and indexes of precipitation and temperature at both annual (between AD 1512 and AD 1911) and decadal (between AD 1000 and AD 1900) scales. Results also show that more locusts can be expected under dry and cold conditions and, in particular, a robust correlation between locust abundance and precipitation is significant at least as far back as AD 500. However, our locust–temperature correlation was weaker and less constant (i.e., it alternated between positive and negative correlations over long timescales), which may reflect the fact that temperature change impacts on outbreaks of oriental migratory locust are indirect and more easily moderated by other factors, such as cooling leading to a decrease in summer monsoonal rainfall

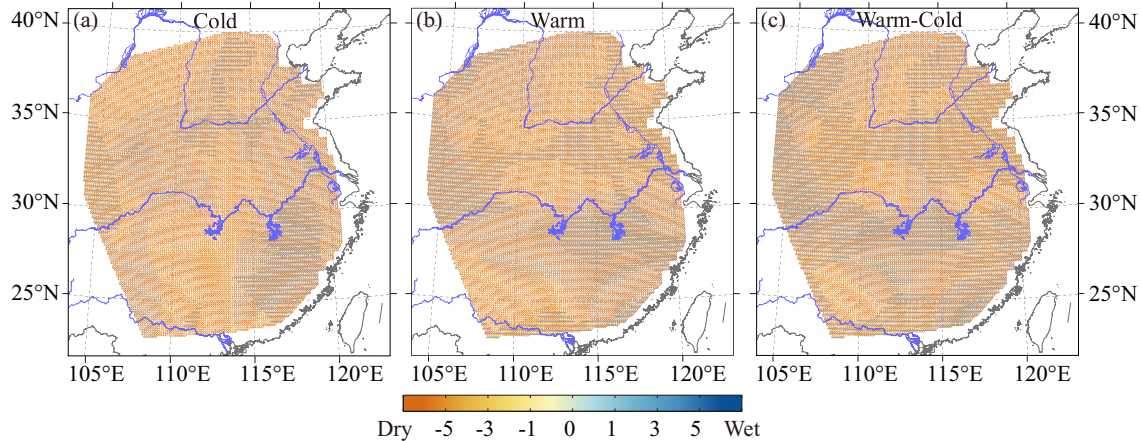


Fig. 4. Ensemble means of dry–wet index spatial patterns for the five cold epochs of AD 440 to AD 540, AD 780 to AD 920, AD 1390 to AD 1460, AD 1600 to AD 1700, and AD 1800 to AD 1900; as well as the four warm epochs of AD 650 to AD 750, AD 1000 to AD 1100, AD 1190 to AD 1290, and AD 1900 to AD 2000. Spatial pattern differences are shown when climate changes from cold to warm (Hao et al., 2016).

via reduced moisture transport from surrounding oceans onto the Asian continent.

Nevertheless, on the basis of spatial and temporal human plague records for China between AD 1850 and AD 1964, there is a significant association between human plague intensity (i.e., cases per year) and the dry–wet index (Xu et al., 2011). Results show, however, that responses to plague intensity under dry versus wet conditions were different in northern and southern China. In the former region, plague intensity generally increased in concert with wetness for both the current and previous year, with the exception of low recorded intensity during extremely wet conditions in the current year (i.e., a dome-shaped response to current year dry–wet index values). In contrast, in southern China, plague intensity generally decreased as wetness increased, with the exception of high intensities during extremely wet conditions in a current year. These opposite effects are likely to be related to differences in climate and rodent communities between these two regions of China; in the arid north, rodents would be expected to respond positively to enhanced precipitation, while in the humid south, high precipitation is likely to have a negative effect.

4. Conclusion

In this paper we report on a number of high-resolution proxies, paleoclimatic reconstructions, and new results through CCCP2k studies attained over the last five years. The following points can be concluded from this work:

(1) Multi-proxy synthesized reconstructions for China show significant cycles in temperature variation over the last 2000 years, including 50–70-yr, 100–120-yr, and 200–250-yr cycles. At the same time, the amplitudes for decadal and centennial variation in temperature are 1.3°C and 0.7°C, respectively, and centennial variation is significantly correlated with long-term changes in solar radiation—especially cold periods, which correspond approximately to sunspot minima, as well as the frequency of large volcanic eruptions. Results further show that the linear warming trend across the whole of China was $0.56 \pm 0.42^\circ\text{C}$ (100 yr) $^{-1}$ for the period between AD 1870 and AD 2000. This was very likely the most rapid in the last 2000 years, although a similar warming rate also occurred in intervals between cold and warm periods before the 20th century. The warmth of the 20th century may not be unprecedented over the last 2000 years; the temperature of two peaks at AD 1080 and AD 1250 during the MCA are comparable.

(2) Spatial patterns in the dry–wet index ensemble mean for eastern China (i.e., the mainland region approximately east of 105°E and south of 40°N) across all centennial warm periods correspond to a tripole pattern of dry conditions south of 25°N, wet conditions between 25°N and 30°N, and dry conditions north of 30°N. In contrast, ensemble mean spatial patterns exhibit an east-to-west distribution for centennial cold periods, with wet conditions dominant east of 115°E and dry conditions prevalent west of 115°E, albeit with a wetness

exception around 110°E. An increase in precipitation in the monsoonal regions of China corresponding with 20th century warming can primarily be attributed to a mega-ENSO (one significant cause of interannual-to-interdecadal variations in global SST), as well as the AMO.

(3) Results show a significant association between the occurrences of locusts, human plagues, and long-term climate variation in eastern China, with more locusts recorded in dry and cold conditions. However, plague intensity responses to changes in wet and dry conditions are different in northern and southern China; plague intensity has generally increased with wetness in northern China, while high precipitation has historically had a negative effect in the south.

These findings reported in this paper may improve our understanding of whether or not the warming observed in the 20th century can be considered exceptional within the past regional context. We have also explored changes in spatial patterns of dryness and wetness, as well as the temporal and spatial occurrences of locusts and plagues in China in response to climate warming, and our results provide insights for successful adaptation in the future. The results presented here will also be useful for further studies regarding the sensitivity of regional climate warming to CO₂ concentrations, as well as climate dynamics, at decadal to centennial scales.

Acknowledgements. This study was supported by the Strategic Priority Research Program of the Chinese Academy of Sciences (Grant No. XDA050800), the Key Program of the Chinese Academy of Sciences (Grant No. KJZD-EW-TZ-G10), and the National Natural Science Foundation of China (Grant No. 41671201 and 91525101).

REFERENCES

- Chen, F., Y. Zhang, X. M. Shao, M. Q. Li, and Z.-Y. Yin, 2016: A 2000-year temperature reconstruction in the Animaqin mountains of the Tibet Plateau, China. *Holocene*, **26**, 1904–1913, doi: 10.1177/0959683616646187.
- Chu, G. Q., Q. Sun, X. H. Wang, M. M. Liu, Y. Lin, M. M. Xie, W. Y. Shang, and J. Q. Liu, 2011: Seasonal temperature variability during the past 1600 years recorded in historical documents and varved lake sediment profiles from northeastern China. *Holocene*, **22**(7), 785–792.
- Chu, G. Q., and Coauthors, 2013: Minor element variations during the past 1300 years in the varved sediments of Lake Xiaolongwan, north-eastern China. *GFF*, **135**(3–4), 265–272, doi: 10.1080/11035897.2013.788550.
- Clette, F., L. Svalgaard, J. M. Vaquero, and E. W. Cliver, 2014: Revisiting the sunspot number: A 400-year perspective on the solar cycle. *Space Sci. Rev.*, **186**(1–4), 35–103.
- Cui, Y. F., Y. J. Wang, H. Cheng, K. Zhao, and X. G. Kong, 2012: Isotopic and lithologic variations of one precisely-dated stalagmite across the Medieval/LIA period from Heilong Cave, central China. *Climate of the Past*, **8**(5), 1541–1550.
- Delaygue, G., and E. Bard, 2011: An Antarctic view of beryllium-10 and solar activity for the past millennium. *Climate Dyn.*, **36**, 2201–2218.
- Duan, K. Q., T. D. Yao, N. L. Wang, B. Q. Xu, and L. G. Thompson, 2012: The unstable Holocene climatic change recorded

- in an ice core from the central Tibetan Plateau. *Scientia Sinica Terra*, **42**(9), 1441–1449. (in Chinese).
- Ge, Q., Z. Hao, J. Zheng, and X. Shao, 2013a: Temperature changes over the past 2000 yr in China and comparison with the Northern Hemisphere. *Climate of the Past*, **9**(3), 1153–1160.
- Ge, Q. S., J. Y. Zheng, X. Q. Fang, Z. M. Man, X. Q. Zhang, P. Y. Zhang, and W.-C. Wang, 2003: Winter half-year temperature reconstruction for the middle and lower reaches of the Yellow River and Yangtze River, China, during the past 2000 years. *Holocene*, **13**(6), 933–940.
- Ge, Q.-S., J.-Y. Zheng, Z.-X. Hao, X.-M. Shao, W.-C. Wang, and J. Luterbacher, 2010: Temperature variation through 2000 years in China: An uncertainty analysis of reconstruction and regional difference. *Geophys. Res. Lett.*, **37**, L03703, doi: 10.1029/2009GL041281.
- Ge, Q. S., J. Y. Zheng, Z. X. Hao, and H. L. Liu, 2013b: General characteristics of climate changes during the past 2000 years in China. *Science China Earth Sciences*, **56**(2), 321–329.
- Ge, Q. S., Z. Hua, J. Y. Zheng, X. Q. Fang, L. B. Xiao, J. Liu, and B. Yang, 2015: Forcing and impacts of warm periods in the past 2000 years. *Chinese Science Bulletin*, **60**(18), 1727–1734. (in Chinese)
- Ge, Q. S., J. Y. Zheng, Z. X. Hao, Y. Liu, and M. Q. Li, 2016: Recent advances on reconstruction of climate and extreme events in China for the past 2000 years. *Journal of Geographical Sciences*, **26**(7), 827–854.
- Hao, Z. X., J. Y. Zheng, Q. S. Ge, and W.-C. Wang, 2011: Historical analogues of the 2008 extreme snow event over central and southern China. *Climate Research*, **50**(2–3), 161–170.
- Hao, Z. X., J. Y. Zheng, Q. S. Ge, and X. Z. Zhang, 2012: Spatial patterns of precipitation anomalies for 30-yr warm periods in China during the past 2000 years. *Acta Meteorologica Sinica*, **26**(3), 278–288.
- Hao, Z. X., D. Sun, and J. Y. Zheng, 2015: East Asian monsoon signals reflected in temperature and precipitation changes over the past 300 years in the middle and lower reaches of the Yangtze River. *PLoS One*, **10**(6), e0131159.
- Hao, Z. X., J. Y. Zheng, X. Z. Zhang, H. L. Liu, M. Q. Li, and Q. S. Ge, 2016: Spatial patterns of precipitation anomalies in eastern China during centennial cold and warm periods of the past 2000 years. *Int. J. Climatol.*, **36**(1), 467–475.
- He, M. H., B. Yang, and N. M. Datsenko, 2014: A six hundred-year annual minimum temperature history for the central Tibetan Plateau derived from tree-ring width series. *Climate Dyn.*, **43**(3–4), 641–655.
- IPCC, 2007: *Climate Change 2007: Impacts, Adaptation and Vulnerability. Contribution of Working Group II to the Fourth Assessment Report of the Intergovernmental Panel on Climate Change*, Parry et al., Eds., Cambridge University Press, Cambridge, United Kingdom and New York, NY, USA, 976 pp.
- IPCC, 2013: *Climate Change 2013: The Physical Science Basis. Contribution of Working Group I to the Fifth Assessment Report of the Intergovernmental Panel on Climate Change*, Stocker et al., Eds., Cambridge University Press, Cambridge, United Kingdom and New York, NY, USA, 1535 pp.
- Lan, Y., Z. X. Hao, and J. Y. Zheng, 2015: Variations of monthly precipitation in rainy season of Beijing since AD1724 derived from the “clear and Rain Records”. *Journal of Chinese Historical Geography*, **30**(2), 41–46, 55. (in Chinese)
- Lean, J. L., 2010: Cycles and trends in solar irradiance and climate. *WIREs Climate Change*, **1**, 111–122.
- Li, J. J., X. M. Shao, Y. Y. Li, and N. S. Qin, 2014: Annual temperature recorded in tree-ring from Songpan region. *Chinese Science Bulletin*, **59**(15), 1446–1458. (in Chinese)
- Liao, H., X. B. Ren, Q. S. Ge, Z. W. Yan, Z. H. Lin, and T. J. Zhou, 2016: Climate warming and its sensitivity to CO₂ concentrations—Progress on “climate sensitivity” group of CAS strategic priority research program “Climate change: Carbon budget and relevant issues”. *Bulletin of Chinese Academy of Sciences*, **31**(1), 134–141. (in Chinese)
- Liu, J., B. Wang, M. A. Cane, S.-Y. Yim, and J.-Y. Lee, 2013: Divergent global precipitation changes induced by natural versus anthropogenic forcing. *Nature*, **493**(7434), 656–659.
- Liu, X. Q., Z. T. Yu, H. L. Dong, and H.-F. Chen, 2014: A less or more dusty future in the Northern Qinghai-Tibetan Plateau? *Sci. Rep.*, **4**, 6672, doi: 10.1038/srep06672.
- Lü, D. R., and Z. L. Ding, 2012: Climate change: Carbon budget and relevant issues. *Bulletin of Chinese Academy of Sciences*, **27**(3), 395–402. (in Chinese)
- Muscheler, R., J. Beer, G. Wagner, C. Laj, C. Kissel, G. M. Raisbeck, F. Yiou, and P. W. Kubik, 2004: Changes in the carbon cycle during the last deglaciation as indicated by the comparison of ¹⁰Be and ¹⁴C records. *Earth and Planetary Science Letters*, **219**, 325–340.
- NRC (National Research Council), 2006: *Surface Temperature Reconstructions for the Last 2, 000 Years*. National Academies Press, Washington, DC, 160 pp.
- PAGES 2k Consortium, 2013: Continental-scale temperature variability during the past two millennia. *Nature Geosci.*, **6**, 339–346.
- Qin, D. H., J. Y. Zhang, C. C. Shan, and L. C. Song, 2015: *China National Assessment Report on Risk Management and Adaptation of Climate Extremes and Disasters*. Science Press, Beijing, 377 pp.
- Shao, X. M., 2012: A preliminary reconstruction of temperature in the eastern Qaidam Basin, northeaster Tibetan Plateau, China. *Quaternary International*, **279**–**280**, 444.
- Steinhilber, F., J. Beer, and C. Fröhlich, 2009: Total solar irradiance during the Holocene. *Geophys. Res. Lett.*, **36**, L19704.
- Sun, L. G., and Coauthors, 2013: Preliminary evidence for a 1000-year-old tsunami in the South China Sea. *Sci. Rep.*, **3**, 1655.
- Tan, M., 2014: Circulation effect: response of precipitation δ¹⁸O to the ENSO cycle in monsoon regions of China. *Climate Dyn.*, **42**(3–4), 1067–1077.
- Tan, M., 2016: Circulation background of climate patterns in the past millennium: Uncertainty analysis and re-reconstruction of ENSO-like state. *Science China Earth Sciences*, **59**(6), 1225–1241.
- Tang, G. L., Y. H. Ding, S. W. Wang, G. Y. Ren, H. B. Liu, and L. Zhang, 2010: Comparative analysis of China surface air temperature series for the past 100 years. *Advances in Climate Change Research*, **1**(1), 11–19.
- Tao, S. C., and Coauthors, 2016: SST variation reconstructed by Sr/Ca ratio from corals around Xisha Islands since 1458. *Proceeding of the 4th Conf. on Earth System Science*, Shanghai, China, S03-O-07. (in Chinese)
- Tian, H. D., L. C. Stige, B. Cazelles, K. L. Kausrud, R. Svarverud, N. C. Stenseth, and Z. B. Zhang, 2011: Reconstruction of a 1,910-y-long locust series reveals consistent associations with climate fluctuations in China. *Proc. Natl. Acad. Sci. USA*, **108**(35): 14 521–14 526.
- Vieira, L. E. A., S. K. Solanki, N. A. Krivova, and I. Usoskin, 2011: Evolution of the solar irradiance during the Holocene.

- Astronomy and Astrophysics*, **531**, A6.
- Wang, B., J. Liu, H.-J. Kim, P. J. Webster, S.-Y. Yim, and B. Q. Xiang, 2013: Northern hemisphere summer monsoon intensified by mega-El Niño/Southern Oscillation and Atlantic Multidecadal Oscillation. *Proc. Natl. Acad. Sci. USA*, **110**(14), 5347–5352.
- Wang, J. L., and B. Yang, 2014: General characteristics of temperature changes during the past 1200 years over the north hemisphere, the continents and China. *Quaternary Sciences*, **34**(6), 1146–1155. (in Chinese)
- Wang, J. L., B. Yang, C. Qin, S. Y. Kang, M. H. He, and Z. Y. Wang, 2014: Tree-ring inferred annual mean temperature variations on the southeastern Tibetan plateau during the last millennium and their relationships with the Atlantic Multidecadal Oscillation. *Climate Dyn.*, **43**(3–4), 627–640.
- Wang, J. L., B. Yang, and F. C. Ljungqvist, 2015: A millennial summer temperature reconstruction for the eastern Tibetan Plateau from tree-ring width. *J. Climate*, **28**(13), 5289–5304.
- Wang, S. W., X. Y. Wen, Y. Luo, W. J. Dong, Z. C. Zhao, and B. Yang, 2007: Reconstruction of temperature series of China for the last 1000 years. *Chinese Science Bulletin*, **52**(23), 3272–3280.
- Xiao, D. M., N. S. Qin, J. J. Li, and Y. Y. Li, 2013: Variations of June air temperature derived from tree-ring records in 1713–2010 in Jinchuan, West Sichuan Plateau, China. *Progressus Inquisitiones de Mutatione Climatis*, **9**(4), 252–257. (in Chinese)
- Xiao, D. M., N. S. Qin, J. J. Li, Y. Y. Li, and L. Mu, 2015: Change of mean temperature from July to September in northeast of western Sichuan Plateau Based tree-ring. *Plateau Meteorology*, **34**(3), 762–770. (in Chinese)
- Xu, L., and Coauthors, 2011: Nonlinear effect of climate on plague during the third pandemic in China. *Proc. Natl. Acad. Sci. USA*, **108**(25), 10 214–10 219.
- Yan, J. H., 2014: Characteristics of climate change in the middle and lower reaches of the Yellow River and Yangtze River of China since 1500 AD. PhD dissertation, University of Chinese Academy of Sciences, 96 pp. (in Chinese).
- Yang, B., A. Braeuning, K. R. Johnson, and Y. F. Shi, 2002: General characteristics of temperature variation in China during the last two millennia. *Geophys. Res. Lett.*, **29**(9), 1324.
- Yang, B., M. H. He, T. M. Melvin, Y. Zhao, and K. R. Briffa, 2013: Climate control on tree growth at the upper and lower treelines: A case study in the Qilian Mountains, Tibetan Plateau. *PLoS One*, **8**(7), e69065.
- Zhang, Y., X. M. Shao, Z.-Y. Yin, and Y. Wang, 2014: Millennial minimum temperature variations in the Qilian Mountains, China: Evidence from tree rings. *Climate of the Past*, **10**(5), 1763–1778.
- Zheng, J. Y., Z. X. Hao, X. Q. Fang, and Q. S. Ge, 2014a: Changing characteristics of extreme climate events during past 2000 years in China. *Progress in Geography*, **33**(1), 3–12. (in Chinese)
- Zheng, J. Y., Z. X. Hao, X. Z. Zhang, H. L. Liu, M. Q. Li, and Q. S. Ge, 2014b: Drought/flood spatial patterns in centennial cold and warm periods of the past 2000 years over eastern China. *Chinese Science Bulletin*, **59**(30), 2964–2971. (in Chinese)
- Zheng, J. Y., Y. Liu, Z. X. Hao, and Q. S. Ge, 2016: Phenological cold/warm events recorded in historical documents and quantitative proxies for winter temperature in Southern China during the past 500 years. *Quaternary Sciences*, **36**(3), 690–701. (in Chinese)
- Zheng, J. Y., M. W. Wu, Q. S. Ge, Z. X. Hao, and X. Z. Zhang, 2017: Observed, reconstructed, and simulated decadal variability of summer precipitation over eastern China. *Journal of Meteorological Research*, **31**(1), 49–60.
- Zhu, H.-F., X.-M. Shao, Z.-Y. Yin, P. Xu, Y. Xu, and H. Tian, 2011: August temperature variability in the southeastern Tibetan Plateau since AD 1385 inferred from tree rings. *Palaeogeography, Palaeoclimatology, Palaeoecology*, **305**(1–4), 84–92.